Biochimie 93 (2011) 583–592

Contents lists available at ScienceDirect

Biochimie

journal homepage: www.elsevier.com/locate/biochi

Research paper

Molecular cloning and biochemical characterization of a myotoxin inhibitor from *Bothrops alternatus* snake plasma

Norival A. Santos-Filho [a,b,*], Carlos A.H. Fernandes [c], Danilo L. Menaldo [b], Angelo J. Magro [c], Consuelo L. Fortes-Dias [d], Maria Inácia Estevão-Costa [d], Marcos R.M. Fontes [c], Camila R. Santos [e], Mário T. Murakami [e], Andreimar M. Soares [a,b,*]

[a] Departamento de Bioquímica e Imunologia, Faculdade de Medicina de Ribeirão Preto, Universidade de São Paulo, FMRP-USP, Ribeirão Preto-SP, Brazil
[b] Departamento de Análises Clínicas, Toxicológicas e Bromatológicas, Faculdade de Ciências Farmacêuticas de Ribeirão Preto, Universidade de São Paulo, FCFRP-USP, Ribeirão Preto-SP, Brazil
[c] Departamento de Física e Biofísica, Instituto de Biociências, Universidade Estadual Paulista, UNESP, Botucatu-SP, Brazil
[d] Diretoria de Pesquisa e Desenvolvimento, Fundação Ezequiel Dias, Belo Horizonte-MG, Brazil
[e] Laboratório Nacional de Biociências, Centro Nacional de Pesquisas em Energia e Materiais, Campinas, São Paulo, Brazil

ARTICLE INFO

Article history:
Received 20 July 2010
Accepted 26 November 2010
Available online 7 December 2010

Keywords:
Phospholipase A_2
Myotoxin inhibitor
cDNA
Protein modeling
Molecular dynamics
Bothrops alternatus
Snake plasma

ABSTRACT

Phospholipases A_2 (PLA_2s) are important components of *Bothrops* snake venoms, that can induce several effects on envenomations such as myotoxicity, inhibition or induction of platelet aggregation and edema. It is known that venomous and non-venomous snakes present PLA_2 inhibitory proteins (PLIs) in their blood plasma. An inhibitory protein that neutralizes the enzymatic and toxic activities of several PLA_2s from *Bothrops* venoms was isolated from *Bothrops alternatus* snake plasma by affinity chromatography using the immobilized myotoxin BthTX-I on CNBr-activated Sepharose. Biochemical characterization of this inhibitory protein, denominated αBaltMIP, showed it to be a glycoprotein with Mr of ~24,000 for the monomeric subunit. CD spectra of the PLA_2/inhibitor complexes are considerably different from those corresponding to the individual proteins and data deconvolution suggests that the complexes had a relative gain of helical structure elements in comparison to the individual protomers, which may indicate a more compact structure upon complexation. Theoretical and experimental structural studies performed in order to obtain insights into the structural features of αBaltMIP indicated that this molecule may potentially trimerize in solution, thus strengthening the hypothesis previously raised by other authors about snake PLIs oligomerization.

1. Introduction

Accidents caused by venomous snakes represent a significant public health problem especially in tropical countries, considering the frequency of occurrence and the mortality they induce [1].

The constitution of snake venoms is complex, containing more than 20 different components and with more than 90% of their dry weight corresponding to proteins. Among the protein content of these venoms, there is a wide variety of enzymes, and the non-protein part is composed by carbohydrates, lipids, metals, amino acids, nucleotides, among other constituents [2].

Phospholipases A_2 (PLA_2s, E.C. 3.1.1.4) are enzymes that catalyze the hydrolysis of 2-acyl ester bonds of 3-sn-phospholipids, releasing free fatty acids and lysophosphatides [3]. These enzymes are widely distributed in nature and are found in the interior and exterior of cells [4], pancreatic secretions [5], inflammatory exudates [6] and arthropod and snake venoms [7].

Independently of their primary catalytic function, the PLA_2s can induce several pharmacological and/or toxic effects, such as myonecrosis, anticoagulation, inhibition of platelet aggregation, neurotoxicity, cardiotoxicity, arterial hypotension, increase of the microvascular permeability and edema formation [8–13]. Besides, PLA_2s are also associated with muscular necrosis, an important local effect induced by some snake venoms, which may lead to permanent loss of tissue and function that may result in the amputation of the affected limb [14].

Considering these factors, several studies have been carried out in search of natural inhibitors of snake venom PLA_2s. Some authors already described the presence of these inhibitors in the plasma of

* Corresponding authors. Departamento de Análises Clínicas, Toxicológicas e Bromatológicas, Faculdade de Ciências Farmacêuticas de Ribeirão Preto, Universidade de São Paulo, FCFRP-USP, Ribeirão Preto-SP, Brazil. Tel.: +55 16 602 4714; fax: +55 16 3602 4725.
E-mail addresses: norival@fcfrp.usp.br (N.A. Santos-Filho), andreims@fcfrp.usp.br (A.M. Soares).

0300-9084/$ – see front matter © 2010 Elsevier Masson SAS. All rights reserved.
doi:10.1016/j.biochi.2010.11.016

mammals as *Didelphis albiventris* [15,16] and *Didelphis marsupialis* [17], in plants as *Withania somnifera* [18], *Cordia verbenacea* [19], *Piper umbellatum* and *Piper peltatum* [20], *Bauhinia forficata* [21], and also in the plasma of snakes [22–25].

Plasma of venomous and non-venomous snakes possesses PLA_2 inhibitory proteins, denominated PLIs [25]. According to several studies, these PLIs are responsible for the natural resistance of snakes against the toxic components of their own venoms, or to those of other species [23,26–29].

The PLA_2 inhibitors can be classified into three types (α, β and γ), according to structural aspects [30]. Nevertheless, their mechanisms of action remain unknown, which incites new structural and functional studies. α-type inhibitors (αPLIs) isolated from the plasma of Crotalinae snakes are acidic glycoproteins constituted of more than two subunits and possess sequential similarity to the carbohydrate recognition domain (CRD) of C-type lectins [31]. At the moment, it is believed that the mechanism by which αPLIs neutralize the toxic effects of snake venom PLA_2s involves the CRD region, particularly CRD4, which recognizes and binds to these enzymes, preventing their enzymatic activity on the cell membrane [32].

The present study reports the isolation of a phospholipase A_2 inhibitory protein from *Bothrops alternatus* snake plasma (αBaltMIP) and also highlights interesting biochemical, structural and functional features related to this molecule.

2. Materials and methods

2.1. Materials

A specimen of *B. alternatus* snake was supplied by the serpentarium of Universidade de São Paulo, Ribeirão Preto. Blood was collected in 0.38% sodium citrate and centrifuged for 10 min at 450× *g* and room temperature for obtainment of the corresponding plasma, which was then lyophilized and stored at −20 °C. Another specimen of the same species was obtained from the serpentarium of Fundação Ezequiel Dias, Belo Horizonte, MG. At the time of sampling, the snake was euthanized with CO_2 before dissection. Liver samples were collected, quickly frozen in liquid nitrogen and stored at −80 °C until RNA extraction. Animal care was in accordance with the guidelines of the Brazilian College for Animal Experimentation (COBEA) and was approved by the Committee for Ethics in Animal Utilization of Universidade de São Paulo (No. 09.1.329.53.3) and IBAMA (No. 11781-1). Activated Sepharose 4B-CNBr and Sephacryl S-200 were purchased from Amersham Pharmacia Biotech (GE-Healthcare) and the oligonucleotides from Gibco BRL. All other reagents used for chemical and biological characterization were acquired from Sigma Chem. Co., BioLab, Gibco BRL or Mediatech.

2.2. Phospholipases A_2 and synthetic peptides

BthA-I-PLA_2, bothropstoxins I and II (BthTX-I and -II) from *Bothrops jararacussu*, piratoxins I and III (PrTX-I and -III) from *Bothrops pirajai* and crotoxin B (CB) from *Crotalus durissus terrificus* were isolated by ion-exchange chromatography on CM-Sepharose using 0.05 M ammonium bicarbonate (AMBIC) buffer, pH 8.0, as previously described [33,34]. Peptides were synthesized by Fmoc chemistry, with native endings by a commercial provider (Chiron Mimotopes, Victoria, Australia or PepMetric Technologies Inc., Vancouver, Canada). Their estimated molecular masses were in agreement with corresponding calculated values, with final purity levels of at least 95% by RP-HPLC analysis. Peptides were kept dry at −20 °C, and dissolved in 0.12 M NaCl, 40 mM sodium phosphate (PBS), pH 7.2, immediately before being tested for their activities. Peptides were derived from the C-terminal region 115–129 of the Lys49 PLA_2 – like BthTX-I (pepBthTX-I = $_{115}$KKYRYHLKPFCKK$_{129}$).

2.3. Purification of the inhibitor

αBaltMIP was isolated from *B. alternatus* blood plasma as follows. *B. jararacussu* BthTX-I (40 μg) was coupled to 10 ml of CNBr-activated Sepharose 4B as described by the manufacturer. It was then settled in a 1.0 × 8.0 cm column and equilibrated with 0.1 M phosphate buffer, pH 7.2. *B. alternatus* plasma (10 ml) was diluted with the same buffer (50 ml, buffer 1) and applied on the column at a flow rate of 2.0 ml/min. Absorbance was recorded at 280 nm and sample was refluxed for 2 h followed by an extensive washing with the same buffer. The PLA_2-bound inhibitor was then eluted with 0.1 M glycine-HCl buffer, pH 2.8 (buffer 2), and the pH of the eluted sample was immediately adjusted to pH 7.0 with 0.5 M Tris–HCl buffer, pH 8.0. The αBaltMIP was desalted and concentrated using a YM-10,000 Amicon membrane by successive washings with 0.05 M AMBIC, pH 8.0, aliquoted in 1.0 ml portions, lyophilized and stored at −20 °C [25,35].

2.4. Biochemical characterization

Polyacrylamide gel electrophoresis was performed in the presence of sodium dodecyl sulfate (SDS–PAGE), following a previously described method [36]. A PPSQ-33A (Shimadzu) automatic sequencer was used for the N-terminal sequencing. The phenylthiohydantoin (PTH) amino acids were identified by comparing their retention times with the 20 PTH-amino acid of the standard mixture. The peptides obtained were compared with the sequences of other related proteins in the SWISS-PROT/TREMBL databases using the FASTA and BLAST programs. To confirm the purity degree, reverse-phase HPLC was performed using a C18 column of 4.6 × 100 mm (GE-Healthcare). C18 column was equilibrated with solvent A (0.1% trifluoroacetic acid), and eluted with a concentration gradient of solvent B (70% acetonitrile, 0.1% trifluoroacetic acid) from 0 to 100%, at a flow rate of 1 ml/min during approximately 90 min. The peaks were monitored by absorbance at 280 nm.

2.5. Inhibitory effect of αBaltMIP on biological activities of snake venom PLA_2s

2.5.1. Inhibition of anticoagulant and PLA_2 activities

The ability of αBaltMIP to inhibit the enzymatic activity of the basic Asp49 PLA_2s BthTX-II, BthA-I-PLA_2, PrTX-III and CB was evaluated by previous incubation of these toxins (25 μg) with the inhibitor at different molar ratios. Anticoagulant activity was assayed on platelet poor plasma and the PLA_2 assay on agarose gel containing red blood cells and egg yolk phospholipids [25,33,37].

2.5.2. Inhibition of cytotoxic activity

Cytotoxicity induced by PLA_2s (20 μg) in the presence or absence of αBaltMIP was assayed on endothelial cells (tEnd) according to Angulo et al. [38]. In order to establish the 100% cytotoxic level for tEnd cells, 150 μl of 0.1% triton X-100 in culture medium were incubated with the cells. For the 0% reference, the culture medium was used alone. After 3 h of incubation at 37 °C, aliquots of 100 μl from the supernatants were assayed for lactate dehydrogenase (LDH) activity according to the Sigma 500 colorimetric method. Results were expressed as the percentage of cytotoxicity relative to LDH released by the detergent alone. In order to measure the cytotoxic activity upon muscular cells, mouse myoblast cell lines (C2C12) were assayed by 3-(4,5-dimethylthiazol-2-yl)-2,5-diphenyltetrazolium bromide (MTT) staining, as described by Mosmann [39]. Cells were disposed in 96-well plates at a density of 1×10^5 cells per well. After 24 h of

culture, the medium was removed and fresh medium, with or without different concentrations of indicated compounds, as pepBthTX-I (100 μg), pepBthTX-I/αBaltMIP (1:1, molar ratio) and αBaltMIP (100 μg), was added to the wells and incubated for 24 h.

2.5.3. Inhibition of myotoxicity

In vivo myotoxic activity was assayed measuring the creatine kinase (CK) levels in mice plasma ($n = 6$, 20–25 g) after i.m. injection of 50 μl of PBS (phosphate buffered saline) alone or PBS containing 50 μg of Asp49 or Lys49 myotoxin, previously incubated with αBaltMIP, into the right gastrocnemius muscle. CK activity was assayed by the CK–UV kinetic kit (Bioclin, Brazil) as instructed by the manufacturer. The activity was expressed in U/l, one unit corresponding to the production of 1 mmol of NADH per minute [40].

2.6. Circular dichroism spectroscopy

CD measurements were carried out in a JASCO model J-810 CD spectropolarimeter equipped with a peltier thermo-controller within a spectral range of 190–260 nm. The experiments were performed at 20 °C using an optical path-length of 1 mm with a 20 nm/min scanning speed and response time of 2 s. Twenty spectra were accumulated, averaged and corrected from the baseline for buffer solution contribution and the resultant spectra were normalized to residual molar ellipticity [θ]. Samples (protein individually and complexes) were analyzed in 5 mM phosphate buffer (pH 7.4) at molar concentration of 10 μM. The enzyme/inhibitor complex was prepared by mixing 1:1 M ratio, followed by incubation for 2 h at 4 °C. All solutions prior to experimentation were centrifuged at 20,000 × *g* for 10 min to remove any aggregates and insoluble particles. Data analysis and deconvolution were conducted using algorithms implemented on the Dychroweb server [41].

2.7. Dynamic light scattering

The dynamic light scattering (DLS) measurements were performed with native αBaltMIP at 4 °C (277 K) and 10 °C (283 K) at the concentration of 1.0 mg ml^{-1} using a DynaPro TITAN equipment (Wyatt Technology). The results were analyzed with the Dynamics v.6.10 software. The data were measured one hundred times in triplicate.

2.8. RNA extraction and cDNA synthesis

Approximately 120 mg of frozen liver of *B. alternatus* was ground to a fine powder with a mortar and pestle in the presence of liquid nitrogen and used for total RNA isolation, following the guanidine thiocyanate-Trizol® method (Invitrogen, USA). RNA integrity was analyzed by electrophoresis of 0.5–2 mg on a 1% agarose gel. Electrophoresis was run at 100 V/cm using TBE (89 mM Tris base, 89 mM boric acid, 2 mM EDTA, pH 8.0) as the running buffer. The gel was examined under UV light, in the presence of ethidium bromide, for the presence of 18S and 28S bands corresponding to ribosomal RNA. cDNA was synthesized from 2 to 5 mg of total RNA by using a cDNA synthesis kit with oligo(dT)12–18 primer, in the presence of dithiotreitol (First-Strand Synthesis kit, Invitrogen, USA). PCR reactions were carried out with specific oligonucleotides designed on the basis of the published nucleotide sequence encoding for the αPLIs from *Trimeresurus flavoviridis* [42]. Amplification conditions were 5 min at 94 °C, 35 cycles of 3 min at 94 °C, 30 s at 55 °C and 30 s at 72 °C, followed by an extension period of 7 min at 72 °C (Perkin Elmer 2400 Thermocycler). A negative control was carried out with no DNA. Aliquots of the amplification reaction were analyzed by electrophoresis on 1.0% agarose gels in TBE buffer, in the presence of ethidium bromide.

2.9. Cloning and cDNA sequence of αBaltMIP

Fresh PCR products were cloned in TA pCR 2.1 plasmid according to manufacturer's instructions (TA Cloning kit, Invitrogen, USA). After transformation of *Escherichia coli* strain INVaF' competent cells, putative positive colonies were confirmed by PCR with αPLIs primers [42]. Five positive clones were randomly selected for growth in liquid culture and the recombinant DNA was purified using a commercial kit (Wizard Plus Minipreps, Promega, USA). DNAs were completely sequenced by the dideoxy chain termination method (Sanger et al., 1977) on an automated ABI Prism 310 Genetic Analyser (Perkin Elmer Applied Biosystem, USA), using M13 forward and M13 reverse oligonucleotides as primers in the Big Dye Terminator Cycle sequencing Ready Reaction (Perkin Elmer Applied Biosystems, CA, USA). The complete cDNA sequences were deposited in the NCBI GenBank (EU421901 to EU421905).

2.10. Selection and alignment of homologous sequences

The sequences homologous to αBaltMIP were obtained from NCBI database (http://www.ncbi.nlm.nih.gov) using the algorithm BLASTP and a BLOSUM45 matrix. The multiple alignment between αBaltMIP sequence and the selected homologue sequences was executed by the program AMAP v.2.2 using default parameters [43].

2.11. Protein modeling

The crystallographic model of lung surfactant protein D (SP-D) from *Homo sapiens* (PDB code 1pwb_chain A) was selected as the best template for the building of the initial theoretical αBaltMIP structural model, according to data obtained from the based-threading method program HHpred [44] (score = 203.9; e-value = 1.1e−32), available at the Max-Planck Institute for Developmental Biology server (http://toolkit.tuebingen.mpg.de/hhpred). The initial theoretical αBaltMIP structural model was generated by the program MODELLER 8v2 [45] using the selected template.

2.12. Molecular dynamics simulation

The αBaltMIP model from program MODELLER 8v2 was submitted to a molecular dynamics (MD) simulation executed by the program GROMACS (Groningen Machine for Chemical Simulation) v.4.0.2 [46,47] in presence of explicit water molecules [48], using an Intel Core 2 Quad ×64 equipped with an Ubuntu v.10.04 Linux operational system. Protonation states of charged groups were set according to pH 7.0. Counter ions were added to neutralize the system and the GROMOS 96 53a6 force field [49] was chosen to perform the MD simulation. The minimum distance between any atom of the protein and the box wall was 1.0 nm. An energy minimization (EM) using a steepest descent algorithm was performed to generate the starting configuration of the system. After this step, 200 ps of MD simulation with position restraints applied to the protein (PRMD) was executed in order to relax the system gently. Then, 10 ns of unrestrained MD simulation were calculated to evaluate the stability of the structures. All the MD simulations were carried out in a periodic truncated dodecahedron box under constant temperature (298 K) and pressure (1.0 bar) maintained by the coupling to an external heat and an isotropic.

2.13. Evaluation of the theoretical αBaltMIP structural models and assembling of the hypothetical oligomeric structure

Overall quality of all the theoretical αBaltMIP models obtained after modeling, MD simulation, and simulated annealing refinement were checked with the programs RAMPAGE [50] and ProSA-web

(https://prosa.services.came.sbg.ac.at/prosa.php) [51]. Average RMSF values of the backbone atoms from the final monomeric αBaltMIP MD model were calculated and converted to B-factor values using the program GROMACS v.4.0.2 [46,47]. The radii of gyration presented by the αBaltMIP model during the MD simulation were also calculated with the program GROMACS v.4.0.2. The assembling of the theoretical trimeric αBaltMIP structure was performed with the program O v.11.0.5 [52] by means of C^{α} atom alignments between the final αBaltMIP MD model and each one of the monomers of the trimeric human lung surfactant protein D (SP-D). A simulated annealing refinement using the program CNS v.1.2 [53] was performed in order to check the feasibility of the theoretical αBaltMIP trimer assembled with the program O v.11.0.5.

2.14. Statistical analysis

Results are presented as mean ± S.D. obtained with the indicated number of animals. The statistical significance of differences between groups was evaluated using Student's unpaired *t*-test and analysis of variance (ANOVA). A P value < 0.05 was considered to indicate significance.

3. Results and discussion

In the present work, an α-type phospholipase A_2 inhibitor (αPLI) was purified from *B. alternatus* snake plasma by an affinity chromatography using BthTX-I, a basic Lys49 PLA_2, coupled on CNBr-activated Sepharose 4B (Fig. 1A). In order to confirm its purity degree, the isolated αPLI, named αBaltMIP, was analyzed by reverse-phase HPLC column and electrophoresis in presence of the reducing agent β-mercaptoethanol (Fig. 1B). The inhibitor appeared as a single polypeptide chain, showing to present a relative molecular weight of 24,000 under reducing conditions (Fig. 1B). Some other αPLIs were purified from a variety of snakes, as *T. flavoviridis* [54], *Agkistrodon blomhoffii* [55], *Atropoides nummifer* [23], *Protobothrops flavoviridis* [24], *Bothrops asper* [32], *Bothrops moojeni* [35] and *B. jararacussu* [25].

The ability of αBaltMIP to inhibit phospholipase A_2 and anticoagulant activity was tested (Fig. 2A and B). The specific activity for each PLA_2 alone was considered as 100%. αBaltMIP was more effective in inhibiting the PLA_2 and anticoagulant activity of BthTX-II and PrTX-III, showing to be less active against the activities induced by crotoxin B and BthA-I-PLA_2.

αBaltMIP inhibited between 38 and 41% of the enzymatic activity of BthTX-II and PrTX-III, respectively, showing maximum inhibition in the proportion of 1:1 PLA_2/PLI (mol/mol) (Fig. 2A). It has been reported that αPLIs isolated from American crotaline snakes are more selective towards basic PLA_2s [22,56], while those of Asian species preferentially interact with acidic PLA_2s [31]. Nevertheless, no evident differences in the amino acid sequences of αPLIs could be ascribed to justify this variation in the inhibitory profiles [56]. Quirós and co-workers [23] proposed that an intra specific specialization of the inhibitor towards particular PLA_2s coevolving in its own venom would seem a more reasonable explanation than an early subdivision of the specificity of these inhibitors in Asian and American crotalines.

As previously mentioned, αBaltMIP presented higher anticoagulant inhibition against BthTX-II and PrTX-III (Fig. 2B). A large number of PLA_2s from snake venoms display anticoagulant activity [57,58]. Some authors suggest that the capacity of PLA_2s to bind and cleave membrane phospholipids indicates that snake venom PLA_2s inhibit blood coagulation through the destruction of pro-coagulating phospholipids, being the catalytic activity of PLA_2s directly responsible for its anticoagulant effects [59,60]. Our results corroborate with this hypothesis, since anticoagulant and catalytic activity showed to be similar.

αBaltMIP was also tested for its capacity in inhibiting PLA_2 cytotoxicity, presenting high inhibition of the cytotoxicity (about 80%) induced by Lys49 PLA_2s (BthTX-I and PrTX-I) (Fig. 2C). Some studies involving Lys49 PLA_2s have demonstrated that the C-terminal region is related to the cytotoxic and bactericidal effects of these proteins [61].

The myotoxicity induced by *Bothrops* Asp49 (BthTX-II and PrTX-III) and Lys49 (BthTX-I and PrTX-I) PLA_2s at an inhibitor:toxin molar ratio of 0.4:1 showed that αBaltMIP presented a strong inhibition of

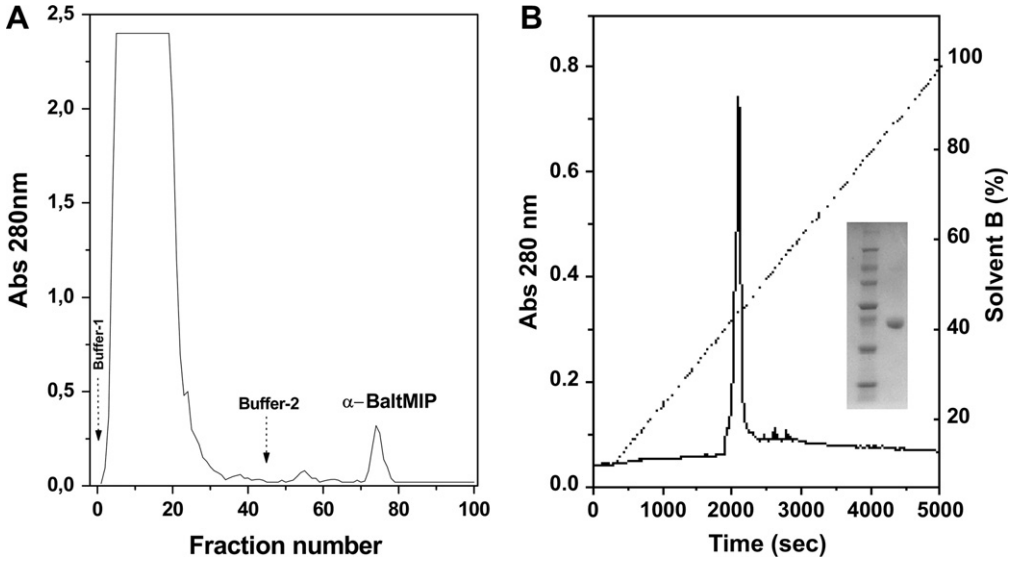

Fig. 1. (A) Purification of the α-type PLA_2 inhibitor from *Bothrops alternatus* snake plasma. *B. alternatus* plasma (~10 ml) was diluted in 50 ml of 0.1 M phosphate buffer, pH 7.2 and applied on a CNBr-activated Sepharose chromatographic column, using a flow rate of 2 ml/min. The inhibitor was eluted with 0.1 M Glycine-HCl, pH 2.8. (B) Evaluation of the purity degree of αBaltMIP by 12% SDS–PAGE (MMW-66,000; 45,000; 36,000; 29,000; 24,000; 20,100; 14,200 and αBaltMIP Mr 24,000) and RP-HPLC using a C18 column and a concentration gradient of solvent B (0–100% of 70% acetonitrile plus 0.1% trifluoroacetic acid).

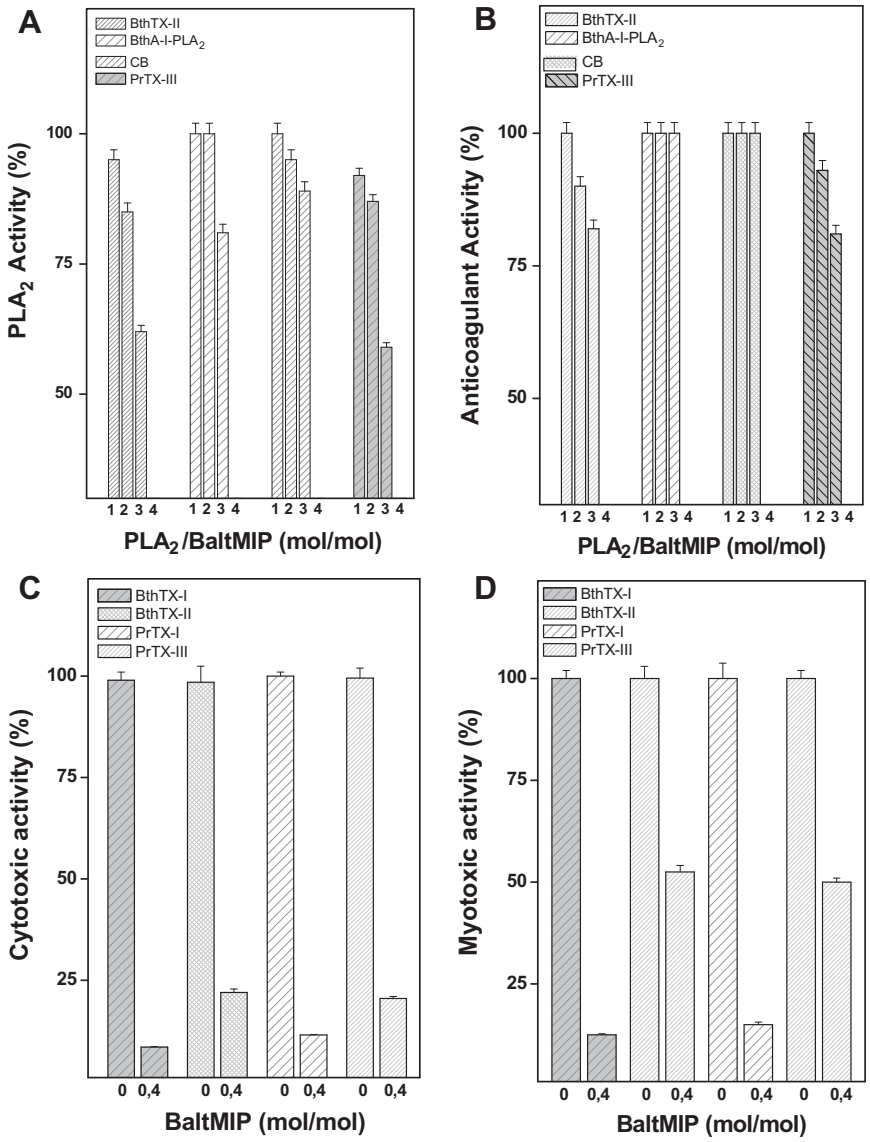

Fig. 2. Inhibitory properties of the αBaltMIP. Inhibition of (A) PLA_2 and (B) anticoagulant activities of isolated PLA_2s from *B. jararacussu*, *B. pirajai* and *Crotalus durissus terrificus* by αBaltMIP (PLA_2/αBaltMIP) at different molar ratios (mol/mol): (1) 1:0.2; (2) 1:0.6; (3) 1:1; (4) 0:1. (C) Neutralization of cytotoxic activity induced by myotoxins BthTX-I, PrTX-I and BthTX-II after incubation with αBaltMIP for 30 min at 37 °C. (D) Neutralization of myotoxic activity of Lys49 and Asp49 myotoxins after incubation with αBaltMIP for 30 min at 37 °C. The total activity of each PLA_2 alone was considered as 100%. Results are expressed as mean ± S.D. ($n = 6$).

about 80% upon Lys49 PLA_2s, and about 40% of inhibition upon Asp49 PLA_2s (Fig. 2D).

According to some authors, the main responsible for the toxic effect in Lys49 PLA_2s is the C-terminal region. This hypothesis could be confirmed by using synthetic peptides belonging to the C-terminal region (amino acids 115–129), which was responsible for the toxic activities of some myotoxic Lys49 PLA_2s [62,63]. This region combines cationic and hydrophobic amino acid residues responsible for the damage mechanism of cellular membranes. The cationic residues can interact with anionic groups of an acceptor site, probably negatively loaded membrane phospholipids [63], while the hydrophobic residues, especially the aromatic ones, can interact with and possibly penetrate the phospholipid bilayer, resulting in its destabilization [62]. However, the fact that a single peptide plays all the main toxic activities of the origin molecule does not prevent the existence of other motifs that can participate or complement the action of the toxic effector site [63].

In contrast, C-terminal peptides of some myotoxic Asp49 PLA_2s showed no membrane direct damage activity, suggesting that the toxic mechanism exercised by these proteins probably involves its catalytic activity as an important step, differently from that used by myotoxic Lys49 PLA_2s [62]. According to this hypothesis, some studies have suggested that myotoxic Asp49 PLA_2s may induce muscle cell damage by affecting the integrity of plasmatic membranes, thereby leading to hyper contraction and other intracellular effects [13,64]. These membranes are formed by different types of phospholipids, mainly phosphatidylcholine, which can be hydrolyzed by Asp49 PLA_2s producing free fatty acids and lysophospholipids, causing cellular damage [13].

In order to bring some light to this discussion, the cytotoxic activity was assayed upon mouse myoblast cell line (C2C12 cells), testing BthTX-I (a Lys49 myotoxin), pepBthTX-I (a synthetic peptide derived from the C-terminal of BthTX-I) and αBaltMIP. The native BthTX-I presented a high cytotoxicity on C2C12 cells, which was

considered as 100%. The synthetic peptide pepBthTX-I also showed cytotoxic activity against the evaluated cell line, even though this activity was less significant (about 76%). When αBaltMIP was previously incubated with BthTX-I and pepBthTX-I, a remarkable reduction on their cytotoxic activity was observed (about 40% of activity to BthTX-I/αBaltMIP and 25% to pepBthTX-I/αBaltMIP, both in the molar ratio of 1:1).

The C-terminal region of Lys49 PLA_2s is possibly responsible for the cytotoxic effect of these enzymes [61–63], and this hypothesis was confirmed by the present work. However, the participation of other regions of the protein in the toxic mechanism cannot be excluded. The interaction between inhibitor and protein (e.g. αBaltMIP/BthTX-I) seems to occur in several ways and not only in the C-terminal region, given that the toxic activity was not abolished using C-terminal synthetic peptides.

As previously mentioned, αBaltMIP was able to inhibit both Lys49 and Asp49 PLA_2 myotoxic/cytotoxic activities, suggesting there might be several ways of inhibition. Soares and co-workers [35] suggested at least two mechanisms through which αPLIs could neutralize PLA_2s: (1) αPLIs could bind to PLA_2 domains via its CRD region and block, through steric hindrance, interaction between the cytotoxic domain and the cell membrane or (2) αPLIs could directly bind to other domains of myotoxins, avoiding direct contact with the membrane.

Furthermore, the secondary structure contents of the Lys49 (BthTX-I) and Asp49 PLA_2s (BthTX-II and CB), the inhibitor αBaltMIP and their respective complexes were analyzed by CD spectroscopy. All three PLA_2s showed characteristic curves of helical proteins featuring well-defined peaks at 208 and 222 nm as expected for a snake venom PLA_2 structure (Fig. 3A). Analogously, the inhibitor CD spectrum indicates a high content of helical structure elements in its structure (Fig. 3A). CD spectra of the PLA_2/inhibitor complexes are considerably different from those corresponding to the individual proteins (Fig. 3B, for more details, see Fig. 3C). Data deconvolution suggests that the complexes had a relative gain of helical structure elements in comparison to the individual protomers (Table 1), which may indicate a more compact structure upon complexation.

The N-terminal sequence of αBaltMIP, comprising the first 31 amino acid residues, was determined by automatic sequencing using the Edman degradation method, showing the sequence HEQDPDGKLLNSLIDALMHLQREFAKLRGAF. The comparison of the N-terminal sequence of αBaltMIP and an amino acid sequence deduced from cDNA of an αPLI from *B. alternatus* (EU421904.1) showed 100% of identity. The deduced mature sequence shows 147 residues, presenting the conserved cysteine residues at positions 64, 119, 133 and 141, and the putative glycosylation site at N103, characteristic of αPLIs (Fig. 4).

Table 1
Data deconvolution of CB, BthTX-I, BthTX-II and their complexes with αBaltMIP, using the CDSSTR method.

	Helix	Strand	Turn	Unordered	Total
CB	0.39	0.14	0.19	0.27	0.99
BthTX-I	0.44	0.17	0.13	0.16	1.00
BthTX-II	0.54	0.12	0.14	0.20	1.00
αBaltMIP	0.50	0.13	0.16	0.22	1.01
Complex1	0.48	0.13	0.16	0.24	1.01
Complex2	0.60	0.15	0.11	0.14	1.00
Complex3	0.55	0.11	0.14	0.20	1.00

Additionally, in an attempt to obtain insights into the structural features of αBaltMIP, a theoretical three-dimensional structure of αBaltMIP was constructed using a threading modeling technique and improved by a 10 ns molecular dynamics (MD) simulation [44–47]. The initial theoretical αBaltMIP structural model calculated by the program MODELLER 8v2 showed a good stereochemical configuration, with 99.3% of its amino acid residues in the favoured and allowed regions of Ramachandran plot [50]. Furthermore, the residues of the initial theoretical αBaltMIP structural model have also presented an adequate overall quality (Z-score = −4.43) in comparison with experimentally-determined native proteins of similar size deposited in the Protein Data Bank (PDB) [51]. The structural characteristics of the initial model are kept in the theoretical αBaltMIP model obtained after a 10 ns molecular dynamics simulation, which presents 97.9% of its residues distributed in the favoured and allowed regions of Ramachandran plot [50] and also an overall good quality (Z-score = −4.99) [51]. The analysis of the overall αBaltMIP structure calculated after the MD simulation showed the two main structural features of αPLIs were conserved at the final model: the α-helical neck and the carbohydrate recognition domain (CRD), whose main secondary structural elements are two α-helices and five β-strains (Fig. 5A).

The comparison of the deduced amino acid sequence of αBaltMIP with other snake αPLIs – including the theoretical model of GbPLIα (an αPLI from *Gloydius brevicaudus*) [65] – and SP-D proteins from *H. sapiens* and *Rattus norvegicus* shows the mammal amino acid

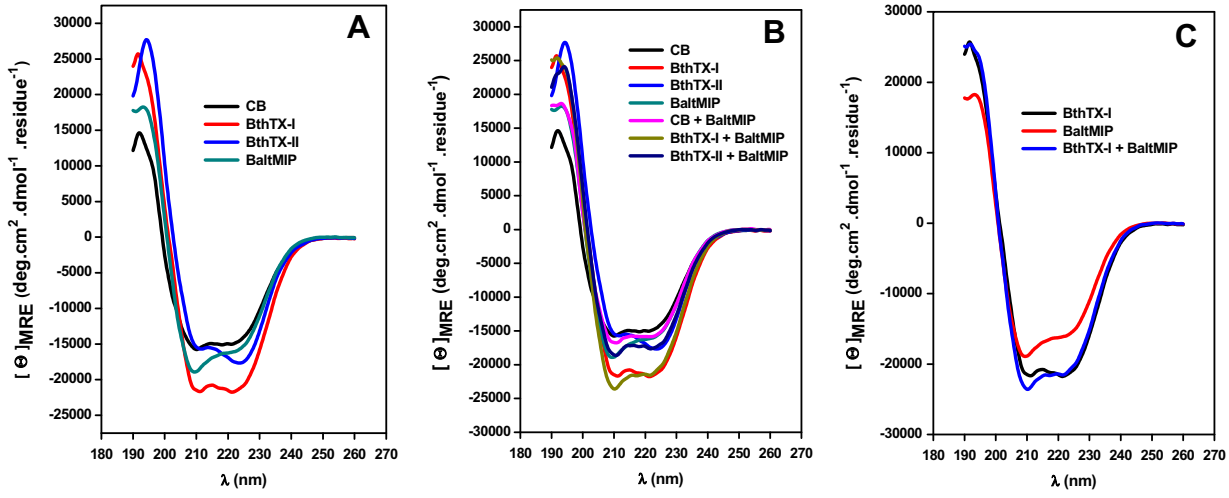

Fig. 3. Far UV-CD spectra for αBaltMIP, PLA_2s and association of PLI/PLA_2. Spectra for CB, BthTX-I, BthTX-II and αBaltMIP alone (A) and for the complexes of these enzymes with αBaltMIP (B); for more details graph (C) presents only BthTX-I and αBaltMIP at a 1:1 M ratio.

```
ATG CGC CTG ATT CTG CTT TCC GGT CTT CTT CTT TTG GGA ATC TTT CTG GCC
 M   R   L   I   L   L   S   G   L   L   L   L   G   I   F   L   A
AAC GGA CAT GAA CAA GAT CCT GAT GGA AAA TTG CTG AAT TCA TTG ATT GAT
 N   G   H   E   Q   D   P   D   G   K   L   L   N   S   L   I   D
GCC CTA ATG CAC CTT CAA AGA GAG TTC GCC AAA CTG AGA GGC GCC TTC CTG
 A   L   M   H   L   Q   R   E   F   A   K   L   R   G   A   F   L
ACA GTC TAC AAA GCC CGA TCC TTT GGG AAT GGC AGT GAA AGA TTG TAC GTG
 T   V   Y   K   A   R   S   F   G   N   G   S   E   R   L   Y   V
ACC AAC AAG GAA ATC AAA AAC TTT GAA GCT CTG AGA CAG ATC TGT GAG CAA
 T   N   K   E   I   K   N   F   E   A   L   R   Q   I   C   E   Q
GCC GGG GGC CAT ATC CCT TCC CCT CAA CTC GAA AAT CAG AAC AAG GCC TTC
 A   G   G   H   I   P   S   P   Q   L   E   N   Q   N   K   A   F
GCA AAT GTT CTG GAG AGG CAC AAC AAA GAA GCC TAC CTT GTT GTG GGT GAC
 A   N   V   L   E   R   H   N   K   E   A   Y   L   V   V   G   D
TCA GCA AAC TTC ACC AAC TGG GCT GCG GGA GAA CCG AAT AAG GCT GCT GGA
 S   A   N   F   T   N   W   A   A   G   E   P   N   K   A   A   G
GCC TGT GTG AAA GCA GAT ACA CAC GGC TCC TGG CAC TCT ACG TCC TGT GAT
 A   C   V   K   A   D   T   H   G   S   W   H   S   T   S   C   D
GAC AAC CTC TTA GTC GTG TGT GAG TTT TAT TTC ATT TTA TGA
 D   N   L   L   V   V   C   E   F   Y   F   I   L   --
```

Fig. 4. cDNA and amino acid sequence of a phospholipase A_2 inhibitor from *Bothrops alternatus* snake plasma (EU421904.1). The underlined amino acids correspond to the N-terminal peptide, which was determined by chemical sequencing of the purified αBaltMIP. The mature polypeptide chain presents 147 amino acid residues.

sequences present an insertion in the 97–109 region (corresponding to 294–306 region according to the human sequence numeration) (Fig. 6). Interestingly, a structural comparison between the final αBaltMIP MD model and the SP-D crystallographic structure from *H. sapiens* indicates this insertion that corresponds to a loop where the residues Asp297 and Glu301 are placed, which are involved in the coordination of two Ca^{2+} ions (Fig. 6). One of these Ca^{2+} ions is also responsible for coordination of important structural elements (a loop and another Ca^{2+} ion) involved in carbohydrate binding [66]. Therefore, the absence of this "Ca^{2+}-binding" loop in the αBaltMIP theoretical model seems to strengthen the hypothesis that snake αPLIs do not bind to carbohydrates and present a Ca^{2+}-independent inhibitory activity, as previously observed by Okumura et al. [65]. In this same work, it was also stated that the α-helical neck regions of snake αPLIs lead to trimerization of these proteins, resulting in the formation of a central pore responsible for binding and inhibition of PLA_2s. Indeed, the dynamic light scattering (DLS) experiments carried out with the purified αBaltMIP strengthen the possible importance of oligomerization for this protein and, possibly, for other snake αPLIs. The DLS data showed αBaltMIP presents a narrow unimodal size distribution at 4 °C (277 K) and 10 °C (283 K), with, respectively, polidispersity values of 3.3% and 13.4% and mean hydrodynamic radii (R_H) of 3.4 nm and 3.6 nm. Remarkably, the R_H values of the scattering centers formed in the tested conditions are considerably distinct from the radius of gyration values (~2.0–2.5 nm) presented by the αBaltMIP model

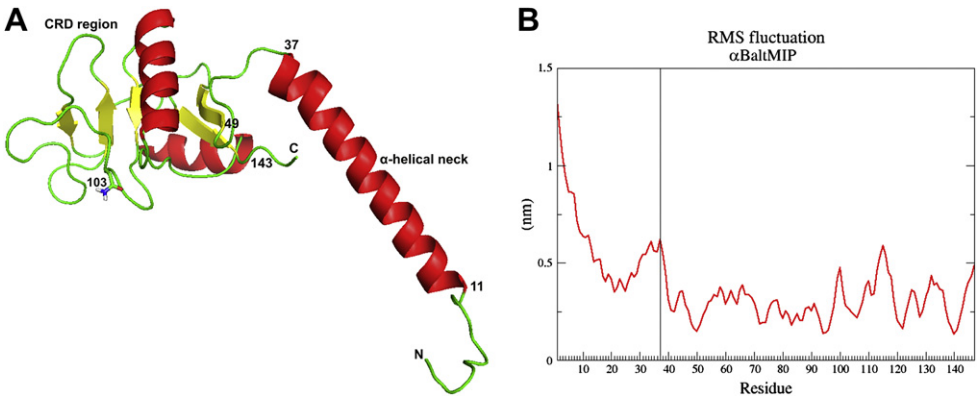

Fig. 5. (A) Cartoon representation of the final theoretical αBaltMIP model obtained after a 10 ns molecular dynamics (MD) simulation [46,47]. The residues 11–37 and 49–143 correspond, respectively, to the α-helical neck region and carbohydrate recognition domain (CRD); the residue Asn103 (stick representation) corresponds to a glycosylation site and it is preserved in all snake αPLI sequences. Illustration generated by the program PyMOL v.1.0 [67]. (B) Average backbone atom RMSF values of the final monomeric αBaltMIP MD model calculated by the program GROMACS v.4.0.2 [46,47]. The vertical line separates the α-helical neck region from the carbohydrate recognition domain (CRD) to emphasize the high flexibility presented by the first segment in comparison to the second during the MD simulation.

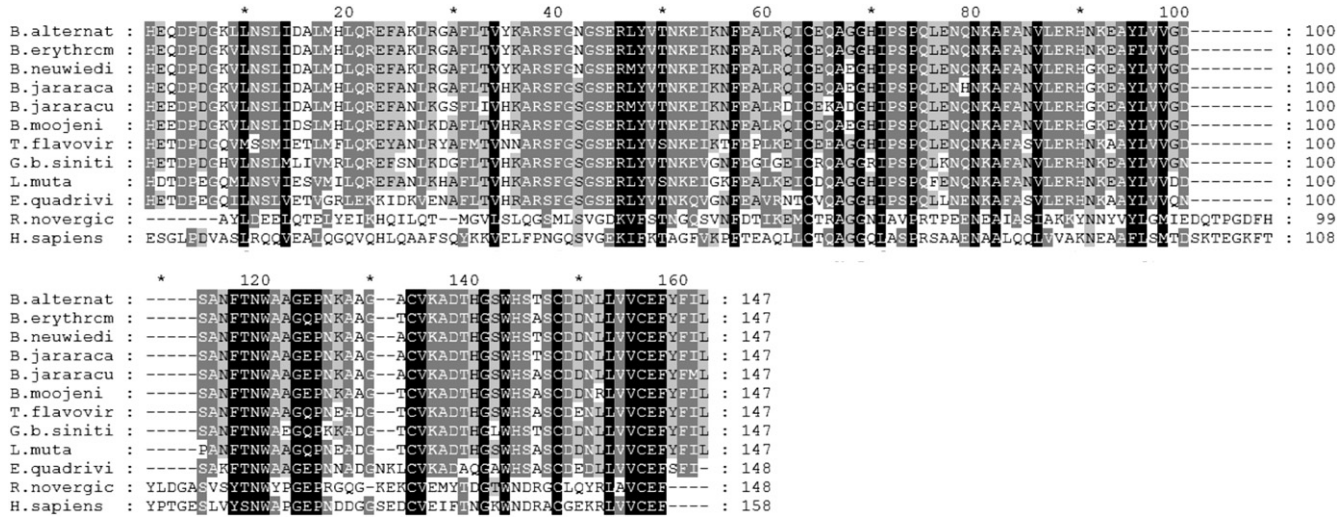

Fig. 6. Multiple alignment between the amino acid sequences of αBaltMIP and other snake αPLI sequences and mammalian lung surfactant proteins D (SP-D) generated with the program AMAP v.2.2 [43]. All the sequences were obtained in the NCBI protein database. αPLIs: *Bothrops alternatus* (gi:215275473); *Bothrops erythromelas* (gi:215275474); *Bothrops neuwiedi* (gi:218546740); *Bothrops jararaca* (gi:215275475); *Bothrops jararacussu* (gi:167547115); *Bothrops moojeni* (gi:218546738); *Gloydius blomhoffii siniticus* (gi:6467183); *Lachesis muta* (gi:218546736); *Trimeresurus flavoviridis* (gi:160357989); *Elaphe quadrivirgata* (gi:82133672). Mammalian lung surfactant proteins D (SP-D): *Rattus norvegicus* (gi:39654792); *Homo sapiens* (gi:34810883).

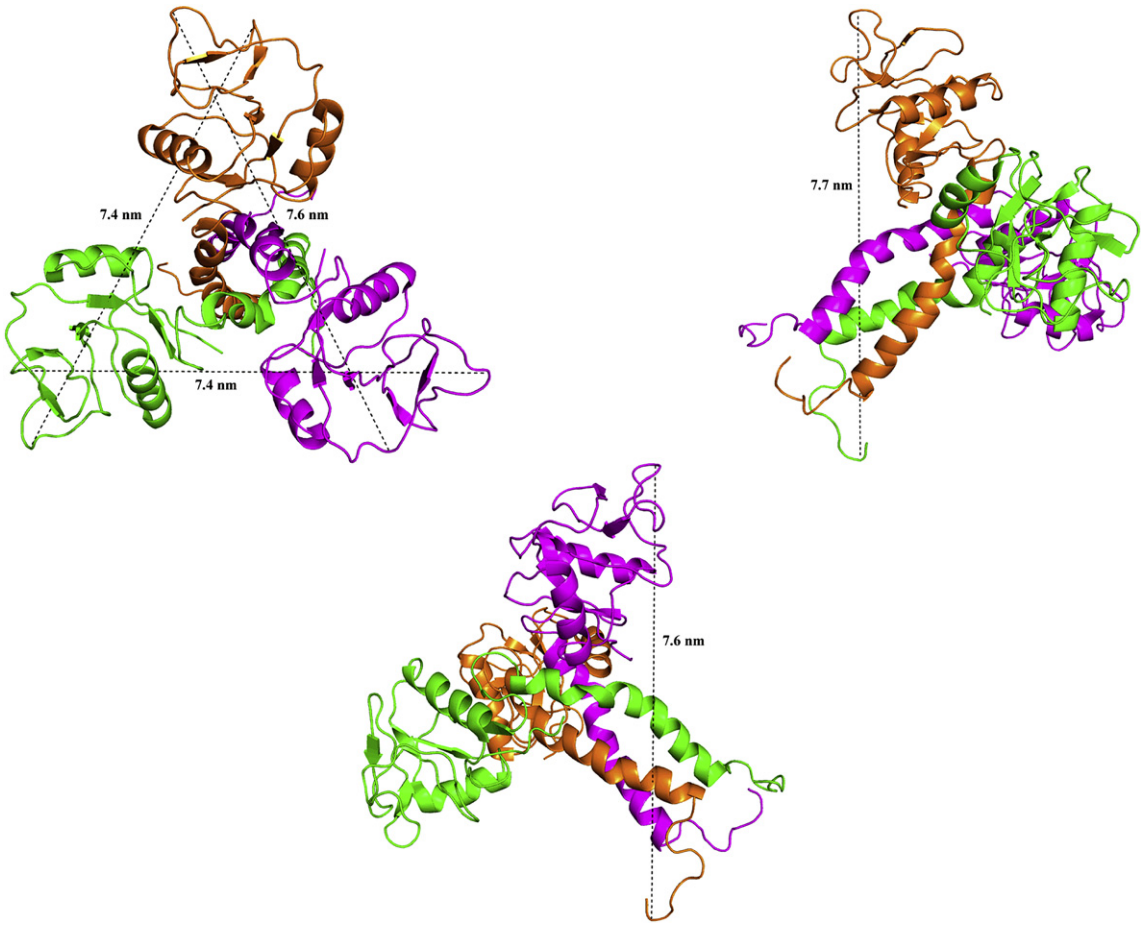

Fig. 7. Hypothetical αBaltMIP trimeric assembling obtained after a simulated annealing refinement [52,53]. The three αBaltMIP monomers fitted well in a trimeric spherical arrangement whose maximum dimensions (about 7.5 nm) indicate that the approximate radius of the oligomer is quite close to the broader R_H value (3.6 nm) calculated in the DLS experiments at 10 °C. It is also possible to observe a slightly twist between the α-helical neck regions, suggesting the probable importance of these regions for the oligomeric assembling. Illustration generated by the program PyMOL v.1.0 [67].

during the MD simulation [46,47]. Hence, since the MD simulation was performed with a single monomer, a trimeric oligomer was assembled and submitted to a simulated annealing refinement [52,53] in order to check specifically if αBaltMIP could also trimerize like other snake αPLIs, as proposed by Okumura et al. [65]. The result of this simulated annealing refinement showed the three αBaltMIP monomers fitted well in a spherical trimeric arrangement whose approximate radius (3.75 nm) is quite close to the R_H value (3.6 nm) calculated in the DLS experiments at 10 °C (Fig. 7). Another interesting feature about the theoretical αBaltMIP trimeric model was a noticeable twist between the α-helical neck regions of the model, thus indicating these parts of the molecule may play an important role in trimerization. Interestingly, the root mean square fluctuation (RMSF) of the backbone atoms from α-helical necks during the MD simulation indicates these regions are highly flexible in relation to other segments of the monomeric molecule (Fig. 5B). This structural feature becomes more evident when the RMSF of each αBaltMIP backbone atom is converted into a B-factor value: the backbone atoms of the α-helical neck region present an average B-factor around 1096.9 $Å^2$, whereas the overall B-factor average is approximately 467.4 $Å^2$ [46,47]. Consequently, a possible αBaltMIP trimeric arrangement held by tight interactions between the α-helical neck regions could present the additional benefit of avoiding potential unfavorable contacts of these segments with unspecific PLA_2 sites in a complex whose molar ratio was 1:1. Otherwise, the circular dichroism (CD) trials have showed that the αBaltMIP/PLA_2 complex is probably more compact in relation to the separated protomers due to the relative increase of helical segments in relation to the separated protomers. This finding indicates that the PLA_2 binding could even induce structural modifications in αBaltMIP and other αPLI protomers to optimize and/or accelerate the formation of intricate inhibitory complexes as that suggested here (formed by one trimeric αPLI oligomer and one PLA_2 molecule). Such hypothesis seems reasonably probable when it is taken into account that the concentration of αPLIs in the snake tissues must be far lower in comparison to the conditions of the experimental procedures performed with the purified αBaltMIP.

Acknowledgements

The authors express their gratitude to Fundação de Amparo à Pesquisa do Estado de São Paulo (FAPESP), Fundação de Amparo à Pesquisa de Minas Gerais (FAPEMIG), Instituto de Ciência e Tecnologia em Toxinas (INCTTox) and Conselho Nacional de Desenvolvimento Científico e Tecnológico (CNPq) for the financial support, and also to Prof. Dr. Auro Nomizo and Isabela Gobbo Ferreira (FCFRP-USP) for their technical support on the cytotoxic activity upon C2C12 cells.

Appendix. Supplementary material

Supplementary materials related to this article can be found online at doi:10.1016/j.biochi.2010.11.016.

References

[1] F.M.O. Pinho, I.D. Pereira, Ofidismo, Revista da Associação Medica Brasileira 47 (2001) 24–29.
[2] E.A. Varanda, M.J.S. Giannini, Bioquímica de venenos de serpentes, , In: Venenos. Aspectos clínicos e terapêuticos dos acidentes por animais peçonhentos (1999) pp. 205–223.
[3] E.A. Dennis, Diversity of group types, regulation and function of phospholipases A_2, J. Biol. Chem. 269 (1994) 13057–13060.
[4] M. Murakami, I. Kudo, Phospholipase A_2, J. Biochem. 131 (2002) 285–292.
[5] A.G. Buckland, E.L. Heeley, D.C. Wilton, Bacterial cell membrane hydrolysis by secreted phospholipases A_2: a major physiological role of human group IIa $sPLA_2$ involving both bacterial cell wall penetration and interfacial catalysis, Biochim. Biophys. Acta 1484 (2000) 195–206.
[6] M.L. Touqui, Alaoui-El-Azher, Mammalian secreted phospholipase A_2 and their pathophysiological significance in inflammatory diseases, Curr. Mol. Med. 1 (2001) 739–754.
[7] R.M. Kini, in: Venom Phospholipase A2 Enzymes: Structure, Function and Mechanism, John Wiley and Sons, Chichester, 1997, pp. 1–28.
[8] J.M. Gutiérrez, B. Lomonte, Phospholipases A_2 myotoxins from *Bothrops* snake venoms, in: Venom Phospholipase A_2 Enzymes: Structure, Function and Mechanism. John Wiley and Sons, 1997, pp. 321–352.
[9] J.B. Harris, B.D. Grubb, C.A. Maltin, R. Dixon, The neurotoxicity of the venom phospholipases A_2, notexin and taipoxin, Exp. Neurol. 161 (2000) 517–526.
[10] S.B. Singh, A. Armugam, R.M. Kini, J. Kandiah, Phospholipase A_2 with platelet aggregation inhibitor activity from *Austrelaps superbus* venom: protein purification and cDNA cloning, Arch. Biochem. Biophys. 375 (2000) 289–303.
[11] C.F.P. Teixeira, E.C.T. Landucci, E. Antunes, M. Chacur, Y. Cury, Inflammatory effects of snake venoms myotoxic phospholipase A_2, Toxicon 42 (2003) 947–962.
[12] A.M. Soares, M.R.M. Fontes, J.R. Giglio, Phospholipase A_2 myotoxins from *Bothrops* snake venoms: structure-function relationship, Curr. Org. Chem. 8 (2004) 1–14.
[13] N.A. Santos-Filho, L.B. Silveira, C.Z. Oliveira, C.P. Bernardes, D.L. Menaldo, A.L. Fuly, E.C. Arantes, S.V. Sampaio, C.C. Mamede, M.E. Beletti, F. Oliveira, A.M. Soares, A new acidic myotoxic, anti-platelet and prostaglandin I_2 inductor phospholipase A_2 isolated from *Bothrops moojeni* snake venom, Toxicon 52 (2008) 908–917.
[14] S.A. Nishioka, P.V. Silveira, A clinical and epidemiologic study of 292 cases of lanceheaded viper bite in a Brazilian teaching hospital, Am. J. Trop. Med. Hyg. 47 (1992) 805–810.
[15] A.M. Soares, V.M. Rodrigues, M.H. Borges, S.H. Andrião-Escarso, O.A.B. Cunha, M.I. Homsi-Brandesburgo, J.R. Giglio, Inhibition of porteases, myotoxins and phospholipases A_2 from *Bothrops* venoms by the heteromeric protein complex of *Didelphys albiventris* opossum serum, Biochem. Mol. Biol. Int. 43 (1997) 1091–1099.
[16] E.P. Trento, O.S. Garcia, A. Rucavado, S.C. França, C. Batalini, E.C. Arantes, J.R. Giglio, A.M. Soares, Inhibitory properties of the anti-bothropic complex from *Didelphis albiventris* serum on toxic and pharmacological actions of metalloproteases and myotoxins from *Bothropos asper* venom, Biochem. Pharmacol. 62 (2001) 1521–1529.
[17] S.L.G. Rocha, B. Lomonte, A.G.C. Neves-Ferreira, G.B. Domont, J.M. Gutiérrez, J. Perales, Functional analysis of DM64 an antimyotoxic protein with immunoglobulin-like structure from *Didelphis marsupialis* serum, Eur. J. Biochem. 269 (2002) 6052–6062.
[18] M. Deepa, T.V. Gowda, Purification and characterization of a glycoprotein inhibitor of toxic phospholipase from *Withania somnifera*, Arch. Biochem. Biophys. 408 (2002) 42–50.
[19] F.K. Ticli, L.I.S. Hage, R.S. Cambraia, P.S. Pereira, A.J. Magro, M.R.M. Fontes, R.G. Stábile, J.R. Giglio, S.C. França, A.M. Soares, S.V. Sampaio, Rosmarinic acid, a new snake venom phospholipase A_2 inhibitor from *Cordia verbenácea* (Boraginaceae): antiserum action potentiation and molecular interaction, Toxicon 46 (2005) 318–327.
[20] V. Nuñez, V. Castro, R. Murillo, L.A. Ponce-Soto, I. Merfort, B. Lomonte, Inhibitory effects of *Piper umbellatum* and *Piper peltatum* extracts towards myotoxic phospholipase A_2 from *Bothrops* snake venoms: isolation of 4-nerolidylcatechol as active principle, Phytochemistry 66 (2005) 1017–1025.
[21] C.Z. Oliveira, V.A. Maiorano, S. Marcussi, C.D. Sant'Ana, C.D. Januário, M.V. Lourenço, S.V. Sampaio, S.C. França, P.S. Pereira, A.M. Soares, Anticoagulant and antifibrinogenolytic properties of the aqueous extract from *Bauhinia forficata* against snake venoms, J. Ethnopharmacol 98 (2005) 213–216.
[22] S. Lizano, G. Domont, J. Perales, Natural phospholipase A_2 myotoxin inhibitor proteins from snakes mammals and plants, Toxicon 42 (2003) 963–977.
[23] S. Quirós, A. Alape-Girón, Y. Angulo, B. Lomonte, Isolation, characterization and molecular cloning of AnMIP, a new alpha-type phospholipase A_2 myotoxin inhibitor from the plasma of the snake *Atropoides nummifer* (Viperidae: Crotalinae), Comp. Biochem. Physiol. B 146 (2007) 60–68.
[24] A. Shimada, N. Ohkura, K. Hayashi, Y. Samejima, T. Omori-Satoh, S. Inoue, K. Ikeda, Subunit structure and inhibition specificity of alpha-type phospholipase A_2 inhibitor from *Protobothrops flavoviridis*, Toxicon 51 (2008) 787–796.
[25] C.Z. Oliveira, D.L. Menaldo, S. Marcussi, N.A. Santos-Filho, L.B. Silveira, J. Boldrini-França, V.M. Rodrigues, A.M. Soares, An alpha-type phospholipase A_2 inhibitor from *Bothrops jararacussu* snake plasma: structural and functional characterization, Biochimie 90 (2008) 1506–1514.
[26] J. Perales, G.B. Domont, Are inhibitors of metalloproteinases, phospholipases A_2 and myotoxins members of the innate immune system. in: A. Ménez (Ed.), Perspectives in Molecular Toxinology. Wiley, Chichester, 2002, pp. 435–456.
[27] G. Faure, Natural inhibitors of toxic phospholipases A_2, Biochimie 82 (2000) 833–840.
[28] C.L. Fortes-Dias, Endogenous inhibitors of snake venom phospholipase A_2 in the blood plasma of snakes, Toxicon 40 (2002) 481–484.
[29] S. Marcussi, C.D. Sant'ana, C.Z. Oliveira, A.Q. Rueda, D.L. Menaldo, R.O. Beleboni, R.G. Stabeli, J.R. Giglio, M.R.M. Fontes, A.M. Soares, Snake venom phospholipase A_2 inhibitors: medicinal chemistry and therapeutic potential, Curr. Top. Med. Chem. 7 (2007) 2328–2339.

[30] M.M. Thwin, R.L. Satish, S.T.F. Chan, P. Gopalakrishnakone, Functional site of endogenous phospholipase A_2 inhibitor from python serum. Phospholipase A_2 binding and anti-inflammatory activity, Eur. J. Biochem. 269 (2002) 719–727.
[31] S. Inoue, A. Shimada, N. Ohkura, K. Ikeda, Y. Samejima, T. Omori-Satoh, K. Hayashi, Specificity of two types of phospholipase A_2 inhibitors from plasma of venomous snakes, Biochem. Mol. Biol. Int. 41 (1997) 529–537.
[32] S. Lizano, B. Lomonte, J.W. Fox, J.M. Gutiérrez, Biochemical characterization and pharmacological properties of an inhibitor of basic phospholipase A_2 myotoxins from the plasma of the snake of *Bothrops asper*, Biochem. J. 326 (1997) 853–859.
[33] S.H. Andrião-Escarso, A.M. Soares, M.R.M. Fontes, A.L. Fuly, F.M.A. Correa, J.C. Rosa, L.J. Greene, J.R. Giglio, Structural and functional characterization of an acidic platelet aggregation inhibitor and hypotensive phospholipase A_2 from *Bothrops jararacussu* snake venom, Biochem. Pharmacol. 64 (2002) 723–732.
[34] A.M. Soares, V.M. Rodrigues, M.I. Homsi-Brandeburgo, M.H. Toyama, F.R. Lombardi, R.K. Arni, J.R. Giglio, A rapid procedure for the isolation of the Lys-49 myotoxin II from *Bothrops moojeni* (caissaca) venom: biochemical characterization, crystallization, myotoxic and edematogenic activity, Toxicon 36 (1998) 503–514.
[35] A.M. Soares, S. Marcussi, R.G. Stábeli, S.C. França, J.R. Giglio, R.J. Ward, E.C. Arantes, Structural and functional analysis of BmjMIP, a phospholipase A_2 myotoxin inhibitor protein from *Bothrops moojeni* snake plasma, Biochem. Biophys. Res. Commun. 302 (2003) 193–200.
[36] U.K. Laemmli, Cleavage of structural proteins during the assembly of the head of bacteriophage T4, Nature 227 (1970) 680–685.
[37] S.H. Andrião-Escarso, A.M. Soares, V.M. Rodrigues, Y. Angulo, C. Diaz, B. Lomonte, J.M. Gutiérrez, J.R. Giglio, Myotoxic phospholipases A_2 in *Bothrops* snake venoms: effect of chemical modifications on the enzymatic and pharmacological properties of bothropstoxins from *Bothrops jararacussu*, Biochimie 82 (2000) 755–763.
[38] Y. Angulo, C.E. Nunez, S. Lizano, A.M. Soares, B. Lomonte, Immunochemical properties of the N-terminal helix of myotoxin II, a lysine-49 phospholipase A_2 from *Bothrops asper* snake venom, Toxicon 39 (2001) 879–887.
[39] T. Mosmann, Rapid colorimetric assay for cellular growth and survival: application to proliferation and cytotoxicity assays, J. Immunol. Methods 65 (1983) 55–63.
[40] R.G. Stábeli, S.F. Amui, C.D. Sant'Ana, M.G. Pires, A. Nomizo, M.C. Monteiro, P.R. Romao, R. Guerr-Sá, C.A. Vieira, J.R. Giglio, M.R.M. Fontes, A.M. Soares, *Bothrops moojeni* myotoxin-II a Lys49-phopholipase A_2 homologue: an example of functional versatility of snake venom proteins, Comp. Biochem. Physiol. C 142 (2006) 371–381.
[41] L. Whitmore, B.A. Wallace, Protein secondary structure analyses from circular dichroism spectroscopy: methods and reference databases, Biopolymers 89 (2008) 392–400.
[42] I. Nobuhisa, M. Deshimaru, T. Chiwata, K. Nakashima, T. Ogawa, Y. Shimohigashi, Y. Fukumaki, Y. Sakaki, S. Hattori, H. Kihara, M. Ohno, Structures of genes encoding phospholipase A_2 inhibitors from the serum of *Trimeresurus flavoviridis* snake, Gene 191 (1997) 31–37.
[43] A.S. Schwartz, L. Pachter, Multiple alignment by sequence annealing, Bioinformatics 23 (2007) 24–29.
[44] J. Söding, A. Biegert, A.N. Lupas, The HHpred interactive server for protein homology detection and structure prediction, Nucleic Acids Res. 33 (2005) 244–248.
[45] M.A. Marti-Renom, A. Stuart, A. Fiser, R. Sánchez, F. Melo, A. Sali, Comparative protein structure modeling of genes and genomes, Annu. Rev. Biophys. Biomol. Struct. 29 (2000) 291–325.
[46] H.J.C. Berendsen, D. van der Spoel, R. van Drunen, GROMACS: a message-passing parallel molecular dynamics implementation, Comput. Phys. Commun. 91 (1995) 43–56.
[47] E. Lindahl, B. Hess, R. van der Spoel, GROMACS 3.0: a package for molecular simulation and trajectory analysis, J. Mol. Model. 7 (2001) 306–317.
[48] H.J.C. Berendsen, J.P.M. Postma, W.F. van Gunsteren, J. Hermans, Interaction models for water in relation to protein hydration. in: B. Pullman (Ed.), Intermolecular Forces. D. Reidel Publishing Company, Dordrecht, 1981, pp. 331–342.
[49] C. Oostenbrink, T.A. Soares, N.F.A. van der Vegt, W.F. van Gunsteren, Validation of the 53A6 GROMOS force field, Eur. Biophys. J. 34 (2005) 273–284.
[50] S.C. Lovell, I.W. Davis, W.B. Arendall III, P.I.W. de Bakker, J.M. Word, M.G. Prisant, J.S. Richardson, D.C. Richardson, Structure validation by Calpha geometry: phi, psi and Cbeta deviation, Proteins: Struct. Funct. Genet. 50 (2003) 437–450.
[51] M. Wiederstein, M.J. Sippl, ProSA-web: interactive web service for the recognition of errors in three-dimensional structures of proteins, Nucleic Acids Res. 35 (2007) W407–W410.
[52] T.A. Jones, M. Bergdoll, M. Kjeldgaard, O: a macromolecule modeling environment. in: C.E. Bugg, S.E. Ealick (Eds.), Crystallographic and Modeling Methods in Molecular Design. Springer-Verlag, New York, 1990, pp. 189–195.
[53] A.T. Brünger, P.D. Adams, G.M. Clore, W.L. DeLano, P. Gros, R.W. Grosse-Kunstleve, J.S. Jiang, J. Kuszewski, M. Nilges, N.S. Pannu, R.J. Read, L.M. Rice, T. Simonson, G.L. Warren, Crystallography and NMR system (CNS): a new software system for macromolecular structure determination, Acta Crystallogr. D 54 (1998) 905–921.
[54] H. Kogaki, S. Inoue, K. Ikeda, Y. Samejima, T. Omori-Satoh, K. Hamaguchi, Isolation and fundamental properties of a phospholipase A_2 inhibitor from the blood plasma of *Trimeresurus flavoviridis*, J. Biochem. 106 (1989) 966–971.
[55] N. Ohkura, S. Inoue, K. Ikeda, K. Hayashi, Isolation and amino acid sequence of a phospholipase A_2 inhibitor from the blood plasma of *Agkistrodon blomhoffii siniticus*, J. Biochem. 113 (1993) 413–419.
[56] S. Lizano, Y. Angulo, B. Lomonte, J.W. Fox, G. Lambeau, M. Lazdunski, J.M. Guitiérrez, Two phospholipase A_2 inhibitors from the plasma of *Cerrophidian (Bothrops) godmani* which selectively inhibit two different group II phospholipase A_2 myotoxins from its own venom: isolation molecular cloning, and biological properties, J. Biochem. 346 (2000) 631–639.
[57] C. Ouyang, C.M. Teng, T.F. Huang, Characterization of snake venom components acting on blood coagulation and platelet function, Toxicon 30 (1992) 945–966.
[58] D.A. Higuchi, C.M.V. Barbosa, C. Bincoletto, J.R. Chagas, A. Magalhaes, M. Richardson, E.F. Sanchez, J.B. Pesquero, R.C. Araujo, J.L. Pesquero, Purification and partial characterization of two phospholipases A_2 from *Bothrops leucurus* (white-tailed-jararaca) snake venom, Biochimie 89 (2006) 1–10.
[59] R.M. Kini, Excitement ahead: structure, function and mechanism of snake venom phospholipase A_2 enzymes, Toxicon 42 (2003) 827–840.
[60] L. Chioato, R. Ward, Mapping structural determinants of biological activities in snake venom phospholipases A_2 by sequence analysis and site directed mutagenesis, Toxicon 42 (2003) 869–883.
[61] T.R. Costa, D.L. Menaldo, C.Z. Oliveira, N.A. Santos-Filho, S.S. Teixeira, A. Nomizo, A.L. Fuly, M.C. Monteiro, B.M. De Souza, M.S. Palma, R.G. Stábeli, S.V. Sampaio, A.M. Soares, Myotoxic phospholipases A_2 isolated from *Bothrops brazili* snake venom and synthetic peptides derived from their C-terminal region: cytotoxic effect on microorganism and tumor cells, Peptides 29 (2008) 1645–1656.
[62] C.E. Núñez, Y. Angulo, B. Lomonte, Identification of the myotoxic site of the Lys49 phospholipase A_2 from *Agkistrodon piscivorus piscivorus* snake venom: synthetic C-terminal peptides from Lys49, but not from Asp49 myotoxins, exert membrane-damaging activities, Toxicon 39 (2001) 1587–1594.
[63] B. Lomonte, Y. Angulo, C. Santamaría, Comparative study of synthetic peptides corresponding to region 115–129 in Lys49 myotoxic phospholipases A_2 from snake venoms, Toxicon 42 (2003) 307–312.
[64] A.L. Fuly, S. Calil-Elias, A.M.B. Martinez, P.A. Melo, J.A. Guimarães, Myotoxicity induced by an acidic Asp-49 phospholipase A_2 isolated from *Lachesis muta* snake venom comparison with lysophosphatidylcholine, Int. J. Biochem. Cell Biol. 35 (2003) 1470–1481.
[65] K. Okumura, A. Ohno, M. Nishida, K. Hayashi, K. Ikeda, S. Inoue, Mapping the region of the α-type phospholipase A_2 inhibitor responsible for its inhibitory activity, J. Biol. Chem. 280 (2005) 37651–37659.
[66] A.K. Shrive, H.A. Tharia, P. Strong, U. Kishore, I. Burns, P.J. Rizkllah, K.B.M. Reid, T.J. Greenhough, High-resolution structural insights into ligand binding and immune cell recognition by human lung surfactant protein D, J. Mol. Biol. 331 (2003) 509–523.
[67] W.L. Delano, The PyMOL Molecular Graphics System. DeLano Scientific, San Carlos, 2002.